



Comparative Collapse Performance Assessment of Bridge Pier under Near-Fault and Long Duration Ground Motions

A.H.M.M. Billah⁽¹⁾, M.R. Kabir⁽²⁾, M. Shahria Alam⁽³⁾

⁽¹⁾ Former PhD Student, School of Engineering, Univ. of British Columbia, Kelowna, BC, Canada V1V 1V7,
E-mail: Muntasir.billah@alumni.ubc.ca

⁽²⁾ M.A.Sc. Student, School of Engineering, Univ. of British Columbia, Kelowna, BC, Canada V1V 1V7,
E-mail: rashedulkabir777@gmail.com

⁽³⁾ Associate Professor, School of Engineering, Univ. of British Columbia, Kelowna, BC, Canada V1V 1V7,
E-mail: shahria.alam@ubc.ca

Abstract

Recent seismic events all around the world have necessitated the seismic response evaluation of highway bridges under long duration ground motion. On the other hand, near-fault ground motions possess some features such as distinctive pulse-like time histories, high peak velocities, high ground displacement, high peak ground acceleration (PGA) to peak ground velocity (PGV) ratio, and a wide range of accelerations in their response spectra. They produce damaging and impulsive effects on structures, which require some special attention. Most of the past studies have investigated the effects of either long duration or near-fault motions separately for different structures. This study aims to investigate whether the long duration motions or near-fault ground motions produce more damaging effects for bridge piers during an earthquake. In this study, the bridge pier considered is located in Vancouver, BC. The bridge pier is designed following a performance-based seismic design guideline. Using 20 long duration motions and 20 near-fault motions, the collapse performance of the bridge pier will be evaluated. Using Incremental dynamic analysis, the collapse capacity of the bridge pier will be evaluated considering uncertainties in ground-motion characteristics and structural modeling. The outcome of this study will provide an insight on the comparative collapse performance of bridge pier under long duration and near-fault ground motion.

Keywords: Long duration motion; Near-fault motion; Collapse capacity; Incremental dynamic analysis



1. Introduction

Every year, billions of dollars are spent worldwide to repair damaged bridges and to construct new ones. History demonstrates the high susceptibility of highway bridges to earthquake damage. Twenty-five percent of bridges were damaged during the Northridge Earthquake in Los Angeles, and six of them collapsed [1]. Around \$190 million was cost to repair the damaged bridges [2]. This clearly indicates the high vulnerability of bridges during seismic events and bridges can be categorized as critical structure [3]. Most of the bridge design guidelines aim to preserve life safety during design earthquake and prevent collapse in an event of rare earthquake. The seismic collapse risk of bridges are in general unknown and the lack of quantitative data makes it difficult to calibrate code and design decision [4]. Bearing the importance collapse safety assessment of structures in mind, researchers have developed various methodologies for seismic collapse assessment of buildings [5, 6] and bridges [7]. Moreover, researches on the collapse safety assessment of bridge structures is inadequate in literature, especially for long duration ground motions. Recent earthquakes such as 2011 Tohoku earthquake, 2010 Chile earthquake, and the 2008 Wenchuan Earthquake showed earthquake of duration approximately 300, 200, and 180 s, respectively [8]. These signifies possibility of higher duration earthquakes in near future.

Large duration ground motions influence the predicted collapse capacity by deteriorating strength and stiffness of structural components due to longer applied loading. Although Hancock and Bommer [9] concluded that there is no direct correlation between duration of motion and structural damage using maximum response as damage measure, Chandramohan et al. [10] argued exclusion of structure deterioration model was the primary cause behind this unclear conclusion. Ou et al. [8] considered Takeda hysteretic model in predicting stiffness degradation and showed lower ductility capacity under long duration ground motions. Since a structure undergoes large inelastic deformation during collapse, predicting the cyclic deterioration of structure components are essential in assessing response under seismic loading. This study aims to assess and compare the seismic collapse performance of a steel reinforced concrete (RC) bridge pier for Vancouver considering maximum drift as the demand parameter under near fault and long duration motion suits. Strength degradation of the bridge pier is accounted for reasonably accurate estimation of the structural collapse response during ground excitations.

2. Design and Geometry of Bridge Piers

The bridge pier considered in this study is a circular reinforced concrete bridge pier located in Vancouver, BC and was seismically designed following Canadian Highway Bridge Design Code, 2010 [11]. The considered bridge is a lifeline bridge as per CHBDC 2010 [11]. In an event of the design earthquake (return period of 475 years), a lifeline bridge needs to remain open for immediate use to all traffic. Therefore, the piers need to be designed to achieve this targeted performance. According to CHBDC 2010, the importance factor of $I=3$ and the response modification factor of $R=3$ were considered for this lifeline bridge. Fig. 1 shows the cross section and elevation of the bridge pier. The diameter of the column designed, D , is fixed to be 1.83 m; the column is reinforced with 48 longitudinal rebars and 16 mm-diameter spirals at 76 mm pitch in the plastic hinge length and 100 mm outside the plastic hinge length with a 50 mm clear cover. The height of the pier is 9.14m with an aspect ratio of 5 which ensured the flexure dominated behavior. A constant mass of 85 ton was applied at the top which represents the weight of the superstructure. The material properties of concrete and steel rebar used in the bridge bents are summarized in Table 1.

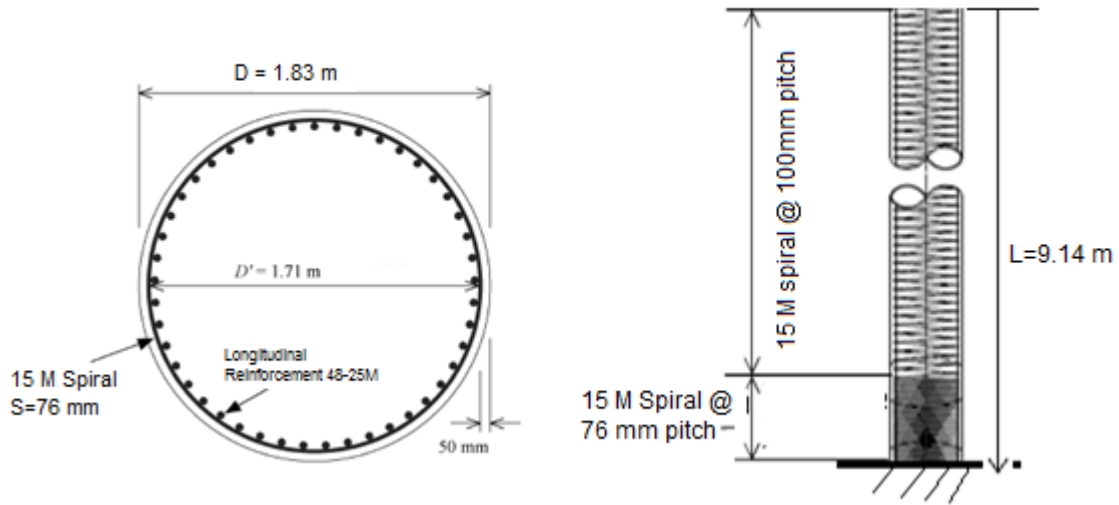


Fig. 1 – Cross section and elevation of reinforced concrete bridge pier

Table 1 – Material properties for reinforced concrete bridge pier

Material	Property	
Concrete	Compressive Strength (MPa)	35
	Corresponding strain	0.0029
	Elastic modulus (GPa)	28.1
Steel	Elastic modulus (GPa)	200
	Yield stress (MPa)	450
	Ultimate stress (MPa)	675
	Ultimate strain	0.14
	Plateau strain	0.016

3. Analytical Modeling of Bridge Pier

Employing an accurate analytical model that incorporates the cyclic deterioration of strength and stiffness is a prerequisite to get a realistic approximation of seismic response under long duration and near fault ground motion. The analytical model should be capable of predicting the expected cyclic and in-cycle deterioration of component strength and stiffness [12, 13]. In this study, a fiber element based nonlinear analysis program SeismoStruct [14] has been employed to evaluate the seismic collapse safety of the bridge pier under near fault and long duration ground motions. Nonlinear static pushover and incremental dynamic analyses (IDA) have been performed to determine the comparative performances of the bridge pier. The program has the ability to figure out the large displacement behaviour, cyclic deterioration, and the collapse load of framed structures accurately under either static or dynamic loading, while taking into account both geometric nonlinearities and material inelasticity [15]. The accuracy of the program in predicting the seismic response of bridge structures has been demonstrated by several researchers through comparisons with experimental results [16, 17, 18].

The bridge pier was modelled using a 3D inelastic beam–column elements, with circular section for the piers by dividing it into number of discrete segments as shown in Fig. 2. The constitutive laws of the reinforcing steel and

of the concrete were, respectively, the Menegotto–Pinto [19] and Mander et al. [20] models. The material models were calibrated to capture the cyclic deterioration to study the effect of ground motion duration. Fig. 3 shows the comparison with experimental result of Sritharan et al. [21] (specimen-IC1). From Fig. 3 it can be observed that the analytical model very well predicts the experimental result and is able to capture the cyclic deterioration. The cumulative energy dissipation was calculated as 46.4 kN m from the predicted load–displacement curve, whereas the experimental result was 50.2 kN m, which is only 7.5% lower than that of the calculated result.

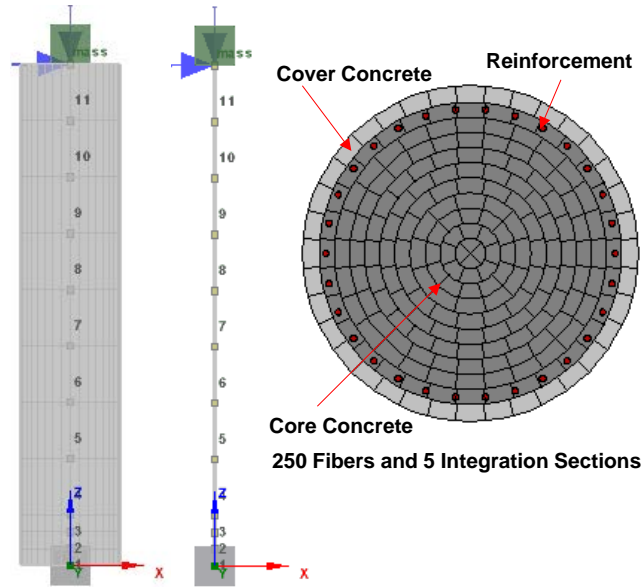


Fig. 2 – Finite element modeling of bridge pier

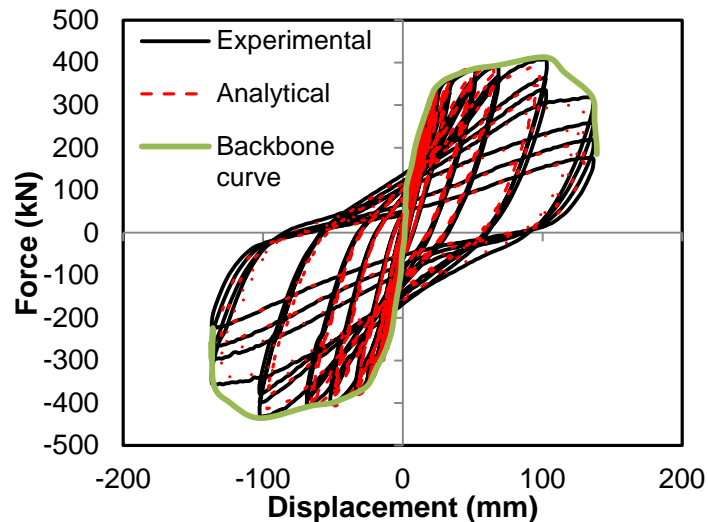


Fig. 3 – Comparison with experimental result to simulate cyclic degradation

4. Collapse Performance Assessment Procedure

The seismic collapse performance of the bridge pier is evaluated for near fault and long duration ground motions following the method developed by Haselton et al. [22]. Incremental dynamic analysis (IDA), a very effective method to predict the behaviour of structures under different levels of ground excitations as predicted by



Vamvatsikos and Cornell [23] was performed in assessing the collapse performance of the bridge pier. The response of the structure such as displacement, acceleration, etc. are observed under scaled ground motion record(s) in this analytical process. Repeated and scaled inelastic time history analysis are performed on the study model until structural collapse occurs in the form of large drift. Structural collapse identified by excessive maximum drift is presented on the basis of input ground motion intensity (spectral acceleration at the first-mode period of the analysis model). In calculating collapse margin ratio, both spectral acceleration at the first-mode period $S_a(T_1)$ and spectrum intensity (SI) could be used effectively as intensity measures for medium period structures [8].

The IDA is repeated for each record in a suite of 20 near fault and 20 long duration ground motions. The near fault ground motion records are obtained from the PEER NGA ground motion database [24] and the long duration records are taken from Center for Engineering Strong Motion Data (CESMD), COSMOS Strong-Motion Virtual Data Center and PEER Strong Motion Database. To account for that uncertainty in frequency content and other characteristics of ground motions, large number of ground motions (20 near fault and 20 long duration ground motions) are used to develop the collapse fragility of the bridge piers. Liel et al. [25] specified this uncertainty as “record-to-record” uncertainty in predicting collapse intensity. The list and characteristics of near fault and long duration ground motions are provided in Table 2 and 3 respectively. The accelerograms were matched to represent the characteristics of structure site. Both the near fault and long duration ground motion record sets are scaled to the design spectrum for Vancouver as per CHBDC 2010 [11]. Fig. 4 demonstrates the response spectra for the two different suits of ground motions. These record sets are systematically scaled to higher intensity until the collapse limit of the bridge pier is reached.

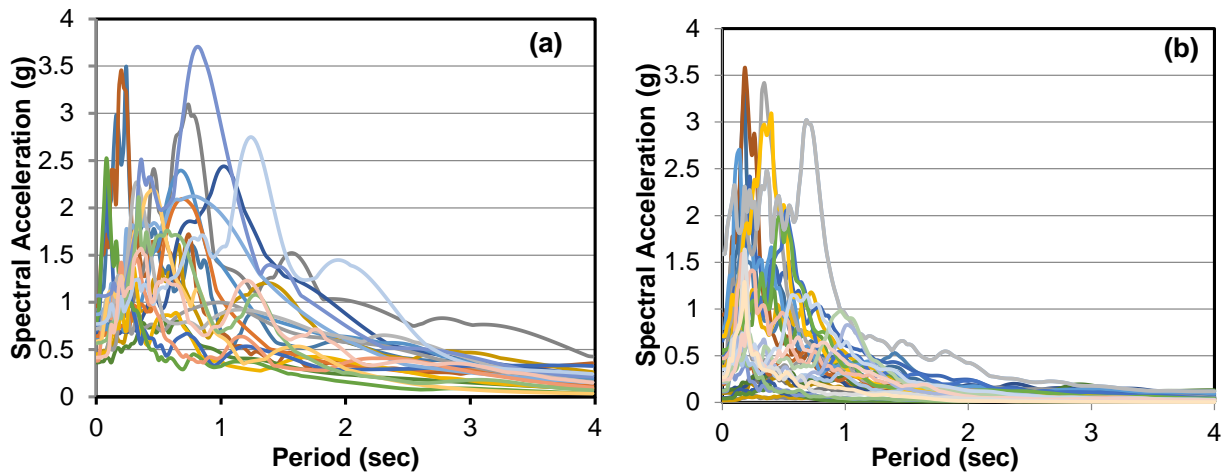


Fig. 4 – Response spectra (a) Near fault and (b) Long duration motions

Table 2 – Characteristics of the near fault ground motion histories

EQ No	Earthquake			Epicentral Distance (km)	PGA (g)	PGV (cm/s.)
	M	Name	Station			
1	7.4	Tabas	-	1.2	0.9	108
2	7.4	Tabas	-	1.2	0.958	103.8
3	7	Loma Prieta	Los Gatos	3.5	0.703	170
4	7	Loma Prieta	Los Gatos	3.5	0.458	89.33
5	7	Loma Prieta	Lex dam	6.3	0.672	175



6	7	Loma Prieta	Lex Dam	6.3	0.37	67.34
7	7.1	Mendocino	Petrolia	8.5	0.625	123.4
8	7.1	Mendocino	Petrolia	8.5	0.65	91
9	6.7	Erzincan	-	2	0.423	117
10	6.7	Erzincan	-	2	0.448	57
11	7.3	Landers	Luc.Valley Stn.	1.1	0.69	133.4
12	7.3	Landers	Luc.Valley Stn.	1.1	0.79	69
13	6.7	Nothridge	Rinaldi	7.5	0.87	171
14	6.7	Nothridge	Rinaldi	7.5	0.381	59.7
15	6.7	Nothridge	Olive view	6.4	0.72	120
16	6.7	Nothridge	Olive view	6.4	0.583	52.9
17	6.9	Kobe	JMA	3.4	1.07	157
18	6.9	Kobe	JMA	3.4	0.563	71
19	6.9	Kobe	Takatori	4.3	0.77	170.5
20	6.9	Kobe	Takatori	4.3	0.424	62.5

Table 3 – List of long duration motions

Event Name	EQ No	Station (Source)	Component	Epi. Dis (km)	PGA (g)	5%-95% Ds (s)
Tohoku, Japan, 2011	1	Sendai (1)	EW	126.1	1.49	106.59
	2	Sendai (1)	NS	126.1	2.31	90.22
	3	Shiogama (1)	EW	118.1	1.49	106.59
	4	Shiogama (1)	NS	118.1	2.31	90.22
	5	Tsukidate (1)	EW	125.9	1.95	85.15
	6	Tsukidate (1)	NS	125.9	4.59	81.5
Valparaiso, Chile, 1985	7	SanIsidro (2)	Long	-	0.69	45.95
	8	SanIsidro (2)	Trans	-	0.38	50.8
	9	Zapallar (2)	EW	-	0.32	45.87
	10	Zapallar (2)	NS	-	0.22	55.09
Maule, Chile, 2010	11	Angol (1)	EW	209.3	0.74	49.76
	12	Angol (1)	NS	209.3	0.95	50.81



	13	Hualane (1)	EW	136	0.38	55.08
	14	Hualane (1)	NS	136	0.37	61.67
	15	Talca (1)	EW	113.1	0.21	72.07
	16	Talca (1)	NS	113.1	0.46	69.86
Sumatra, Indonesia, 2007	17	Sikuai Island (1)	EW	392.2	0.12	42.37
	18	Sikuai Island (1)	NS	392.2	0.12	40.22
ChiChi, Taiwan, 1999	19	CHY025 (3)	EW	-	0.16	97.12
	20	CHY025 (3)	NS	-	0.15	97.15

- (1) Center for Engineering Strong Motion Data (CESMD)
- (2) COSMOS Strong-Motion Virtual Data Center
- (3) PEER Strong Motion Database

5. Characterization of Performance Limits

The seismic collapse safety of the bridge pier is compared using the long duration and near fault record sets. In order to compare the relative collapse safety, the collapse limit state needs to be defined in terms of engineering performance criteria. In this study, various quantitative performance limits (cracking, yielding, strength degradation) corresponding to different drift levels are developed and utilized for analyzing their comparative seismic response under long duration and near fault record sets.

In this study, three quantitative performance limit states were defined for the bridge pier in terms of maximum drift (%). These limit states were developed based on the performance and functional level proposed by Hose et al. [26]. Table 4 shows the three performance limit states and their associated drift limits developed in this study. The performance limit states considered here are, the drift (%) at the onset of longitudinal rebar yielding, cover concrete spalling, and crushing of core concrete.

Table 4 – Damage states of reinforced concrete bridge pier in terms of performance criteria

Performance Level	Functional Level	Description	Drift, Δ (%)
			Steel-RC
Yielding	Operational	Theoretical first yield of longitudinal rebar	$\Delta > 1.42$
Initiation of Local Mechanism	Life safety	Onset of concrete spalling	$\Delta > 1.88$
Strength Degradation	Collapse	Crushing of core concrete	$\Delta > 3.90$

In order to determine the limit state drift values for these performance criteria, the drift limits corresponding to the strain values were determined using a regular push-over analysis. Fig. 5 shows the pushover response curves of the bridge pier and the performance points. The drift limits for the quantitative limit states are provided in Table 4.

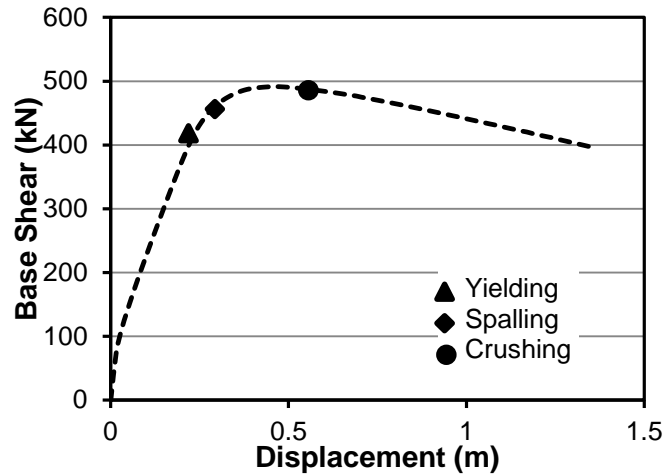


Fig. 5 – Pushover response curve for reinforced concrete bridge piers

6. Seismic Collapse Assessment

Collapse performance of the bridge can be evaluated on the results acquired from incremental dynamic analysis. Several performance parameters such as the median collapse capacity, the collapse margin ratio, and the mean annual frequency of collapse are used in assessing the seismic collapse performance [25]. The median collapse capacity is defined by the spectral intensity when half of the ground motions cause the structure to collapse and depends on the fundamental period of the bridge pier [27]. The collapse margin ratio (CMR) is calculated by the ratio between the median collapse capacity of the structure to the spectral acceleration at maximum considered earthquake (MCE) level (i.e., $S_a(T1)$ for 2% probability of exceedance in 50 years given by seismic design codes). Integration of the collapse fragility function with a site specific hazard curve determines the mean annual frequency of collapse. Only the first two performance parameters are used in this study to compare near fault and long duration ground motions effect on collapse capacity of the bridge pier.

Collapse fragility curve demonstrates the relation between collapse probability and ground motion intensity, which can be derived considering the lognormal distribution of the demand parameter. The collapse fragility curve is derived from the IDA results using the Eq. (1).

$$P(\text{collapse}|S_a) = \Phi\left(\frac{\ln(S_a) - \ln(S_a^C_{50\%})}{\beta_{tot}}\right) \quad (1)$$

where $\Phi(\cdot)$ is the cumulative normal distribution function, $S_a^C_{50\%}$ is the median capacity determined from IDA, and β_{tot} is the total uncertainty. Combining record-to-record and modeling uncertainty, the total uncertainty is calculated using the following equation.

$$\beta_{tot} = \sqrt{\beta_{rtr} + \beta_{model}} \quad (2)$$

where, β_{rtr} is the uncertainty due to the record-to-record variability and the typical value is between 0.35 and 0.45 [25]. β_{rtr} is taken as 0.40 in this study as suggested by ATC-63 [28] and modeling uncertainty (β_{model}) is assumed 0.5 [5].

To evaluate the collapse performance of the bridge pier IDA curves were developed using $S_a(T1,5\%)$ as the IM and maximum drift (%) as the demand parameter. Fig. 6 shows the IDA curves for the bridge pier obtained using the near fault and long duration motions. Since there are number of ground motions used in the IDA, the results are summarized using the EDP given IM (i.e., EDP|IM) percentiles [23]. The IDA results are summarized in median (50% percentile), 16%, and 84% percentiles. With the assumption of a lognormal distribution of maximum drift ratio as a function of $S_a(T1)$, the median (i.e., 50% percentile) is the natural



‘central value’ and the 84%, 16% percentiles correspond to the median times $e^{\pm\text{dispersion}}$, where ‘dispersion’ is the standard deviation of the logarithms of the values [29].

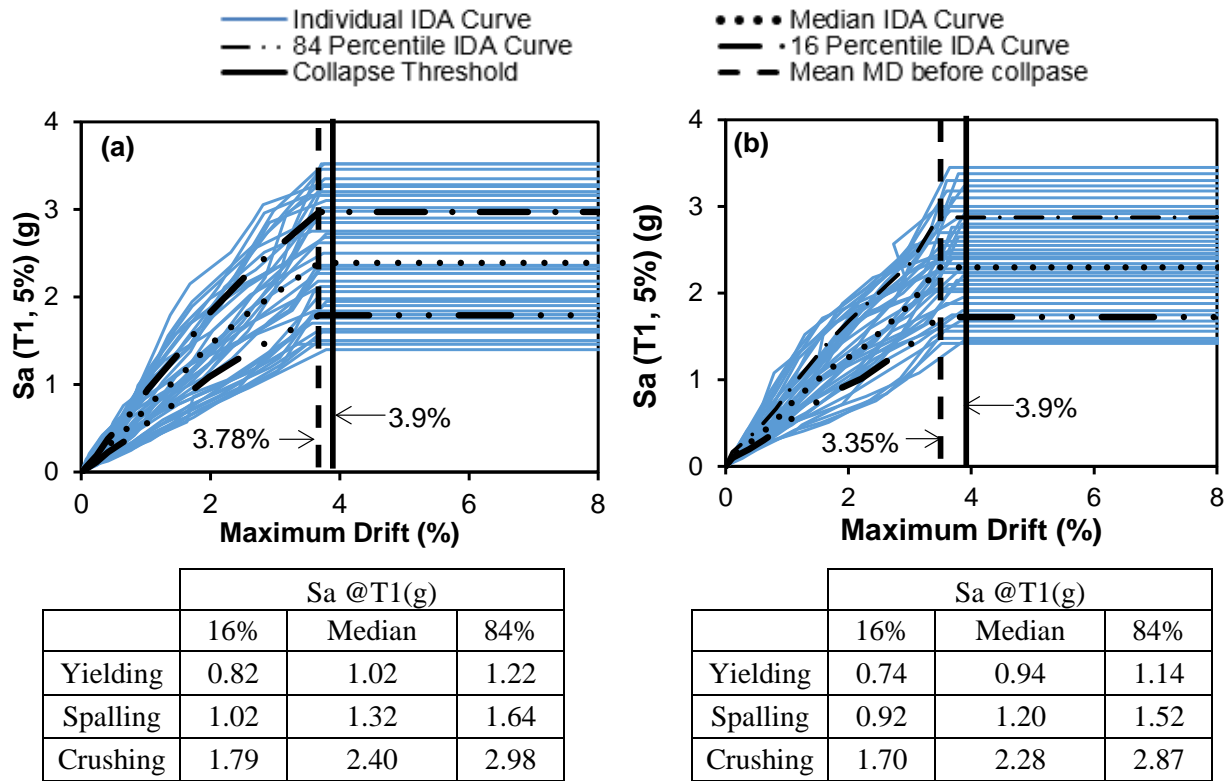


Fig. 6 – IDA curves for maximum drift for reinforced concrete bridge bent pier (a) near fault ground motion (b) long duration motion

Fig. 7a and 7b show the IDA curves for the bridge pier and the percentile results for different limit states under near fault and long duration motions, respectively. From this figure it can be seen that the median S_a at yielding is 1.02g for near fault motion and 0.94g for long duration motion. Similar observation can be made for concrete crushing where the median S_a for near fault and long duration motions are 2.40g and 2.28g, respectively. These figures also show the maximum drift threshold of 3.90% (solid vertical line) which is used to indicate collapse of the bridge pier. From Fig. 8 it can be seen that the near fault ground motions on an average produce a maximum drift of 3.78% just before collapse (dashed vertical line), compared to 3.35% produced by the long duration ground motions. This can be attributed to the large inelastic deformation caused by cyclic deterioration and ratcheting [30, 10] resulting from long duration motion.

Using the IDA results and Eq. (2), the collapse fragility for the bridge pier was developed for two sets of ground motions. Fig. 7 shows the collapse fragility curves for the bridge pier when maximum drift is considered as the performance measure. This figure also shows the median collapse level intensity (S_{CT}) at which 50% of the ground motions cause the bridge pier to collapse.

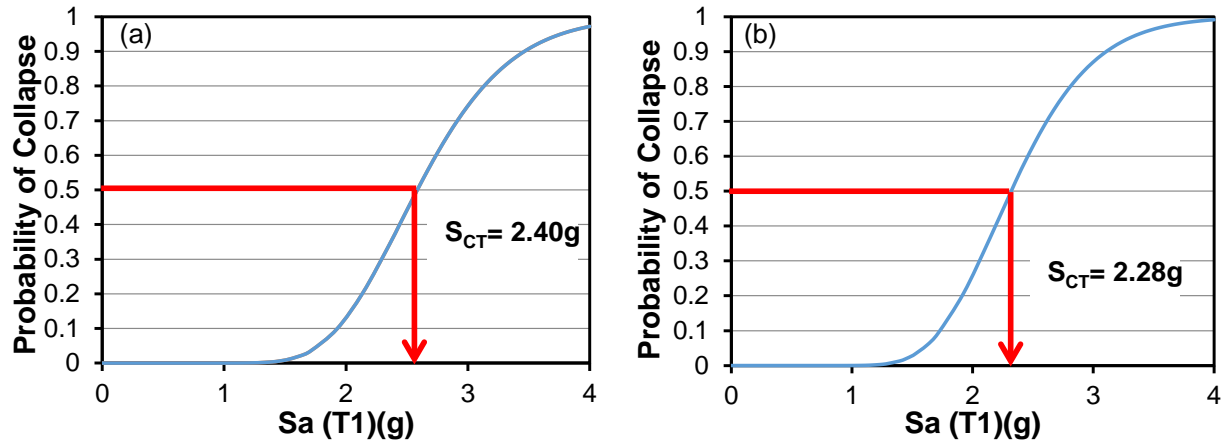


Fig. 7 – Collapse fragility curves for reinforced concrete bridge pier (a) near fault ground motion (b) long duration motion

7. Results

Collapse performance of the bridge pier under near fault and long duration ground motions are summarized in Table 5. The maximum drift (%) ratio ($MD_{collapse}$) along with the collapse performance intensity measures are tabulated here.

Table 5 – Results of collapse performance assessment

	Maximum Drift	
	Near Fault	Long Duration
Fundamental Period, T (sec)	0.48	0.48
Median Collapse Intensity, S_{CT} (g)	2.40	2.28
MCE Demand Intensity, S_{MT} (g)	0.65	0.65
Collapse Margin Ratio (CMR)	3.69	3.50
$MD_{collapse}$ (%)	3.78	3.35

When compared on maximum drift (%), Table 5 shows that long duration ground motion induces lower collapse margin ratio compared to near fault ground motions. 3.69% maximum drift occurs in the bridge pier just before collapse in case of near fault ground motions which is 12.84% higher than long duration ground motions. This is a clear indication of higher plausibility of collapse during long duration earthquake due to cyclic reduction in strength. Regarding near fault suits, the CMR for of the bridge pier designed for Vancouver is 5.43% larger than that of long duration motions. Since a single bridge pier is examined for varying ground motion suits, the median collapse intensity (S_{CT}) portrays the CMR. Lower CMR for long duration motions represent higher likelihood of collapse of the bridge pier.

8. Conclusions

Collapse safety of a steel reinforced bridge pier is assessed in this study by designing it for Vancouver and analysing it under two different suits of motions, near fault and long duration. The performance of the pier is analyzed using collapse margin ratio which is a direct indication of collapse capacity of structure. Maximum



drift (%) is considered as demand parameter in finding collapse intensities. The following conclusions can be drawn based on the numerical results:

1. The steel reinforced RC bridge pier is capable to withstand higher maximum drift before collapse during near fault ground motions than long duration ground motions. Higher number of cyclic loading and longer duration incur cyclic deterioration in strength allowing quicker collapse of the pier.
2. The CMR is slightly lower (5.43%) for long duration ground motion suit indicating higher collapse probability of bridge pier.
3. Median collapse intensity is also showing similar performance for the two suits of ground motions. Near fault ground excitations hold 50% probability of collapse at spectral acceleration 2.40g. Whereas, long duration ground motion suit shows the same probability of collapse at 5% lower spectral acceleration magnitude.
4. This collapse performance assessment study clearly indicates the higher susceptibility of bridge columns towards long duration ground motions. Longer duration of ground shaking degrade the stiffness of the column leading to somewhat lower collapse capacity.

5. References

- [1] Basöz N, Kiremidjian AS, King S.A., Law KH (1999): Statistical analysis of bridge damage data from the 1994 Northridge, CA, earthquake. *Earthquake Spectra*, **15** (1), 25-54.
- [2] Caltrans (1994): Initial and supplementary bridge reports for the Northridge Earthquake. California Department of Transportation. Sacramento, CA.
- [3] Cruz NC, Saïidi MS (2012): Shake-table studies of a four-span bridge model with advanced materials. *Journal of Structural Engineering*, **138** (2), 183-192.
- [4] Liel A, Haselton C (2009): Lessons learned from seismic collapse assessment of buildings for evaluation of bridge structures. *ASCE TCLEE 2009 Lifeline Earthquake Engineering in a Multi-Hazard Environment*, Oakland, California.
- [5] Haselton CB, Deierlein GG (2007): Assessing seismic collapse safety of modern reinforced concrete frame buildings. *Technical Report PEER Report 2007/08*, Pacific Earthquake Engineering Research Center, Berkeley, USA.
- [6] Liel AB, Deierlein GG (2008): Assessing the collapse risk of California's existing reinforced concrete frame structures: metrics for seismic safety decisions. *Technical Report No. 166*, Blume Earthquake Engineering Center, USA.
- [7] Billah AHMM, Chaudhury A, Alam MS (2014): Seismic collapse safety of Shape memory alloy reinforced concrete bridge piers. *CSCE 2014 4th International Structural Specialty Conference*, Halifax, NS.
- [8] Ou Y, Song J, Wang P, Adidharma L, Chang K, Lee GC (2014): Ground motion duration effects on hysteretic behavior of reinforced concrete bridge columns. *Journal of Structural Engineering*, **140** (3), 04013065.
- [9] Hancock J, Bommer JJ (2006): A state-of-knowledge review of the influence of strong-motion duration on structural damage. *Earthquake Spectra*, **22** (3), 827.
- [10] Chandramohan R, Lin T, Baker JW, Deierlein GG (2013): Influence of ground motion spectral shape and duration on seismic collapse risk. *10th International Conference on Urban Earthquake Engineering*, Tokyo, Japan.
- [11] *Canadian highway bridge design code*, 2010. CAN/CSA-S6-10. National Research Council of Canada, Ottawa; ON.
- [12] Ibarra LF, Medina RA, Krawinkler H (2005): Hysteretic models that incorporate strength and stiffness deterioration. *Earthquake Engineering and Structural Dynamics*, **34** (12), 1489-1511.
- [13] Lignos DG, Krawinkler H (2011): Deterioration modeling of steel components in support of collapse prediction of steel moment frames under earthquake loading. *Journal of Structural Engineering*, **137** (11), 1291-1302.
- [14] SeismoSoft, 2015. *SeismoStruct - A computer program for static and dynamic nonlinear analysis of framed structures*, V 7 [online], available from URL: www.seismosoft.com.
- [15] Pinho R, Casarotti C, Antoniou S (2007): A comparison of single-run pushover analysis techniques for seismic assessment of bridges. *Earthquake Engineering and Structural Dynamics*, **36** (10), 1347-1362.



- [16] Casarotti C, Pinho R (2006): Seismic response of continuous span bridges through fibre-based finite element analysis. *Journal of Earthquake Engineering and Engineering Vibration*, **5** (1), 119-131.
- [17] Billah AHMM, Alam MS (2012): Seismic performance of concrete columns reinforced with hybrid shape memory alloy (SMA) and fiber reinforced polymer (FRP) bars. *Construction and Building Materials*, **28** (1), 730-742
- [18] Billah AHMM, Alam MS, Bhuiyan AR (2013): Fragility analysis of retrofitted multi-column bridge bent subjected to near fault and far field ground motion. *ASCE Journal of Bridge Engineering*, **18** (10), 992-1004.
- [19] Menegotto M, Pinto PE (1973): Method of analysis for cyclically loaded R.C. plane frames including changes in geometry and non-elastic behaviour of elements under combined normal force and bending. *Symposium on the Resistance and Ultimate Deformability of Structures Acted on by Well Defined Repeated Loads*, International Association for Bridge and Structural Engineering, Zurich, Switzerland, 15-22.
- [20] Mander JB, Priestley MJN, Park R (1988): Theoretical stress-strain model for confined concrete. *Journal of Structural Engineering*, **114** (8), 1804-26.
- [21] Sritharan S, Priestley MJN, Seible F (1996): Seismic response of column/cap beam tee connections with cap beam prestressing, *Report No. SSRP-96/09*, Structural Systems Research Project, San Diego.
- [22] Haselton CB, Liel AB, Deierlein GG, Dean BS, Chou JH (2011): Seismic collapse safety of reinforced concrete buildings I: assessment of ductile moment frames. *Journal of Structural Engineering*, **137**, 481-492
- [23] Vamvatsikos D, Cornell CA (2002): Incremental dynamic analysis. *Earthquake Engineering and Structural Dynamics*, **31** (3), 491-514.
- [24] PEER (2011). New Ground Motion Selection Procedures and Selected Motions for the PEER Transportation Research Program. *PEER Report 2011/03*, Pacific Earthquake Engineering Research Center, Berkeley, California.
- [25] Liel AB, Haselton CB, Deierlein GG (2011): Seismic collapse safety of reinforced concrete buildings. ii: comparative assessment of nonductile and ductile moment frames. *Journal of Structural Engineering*, **137** (4), 492-502.
- [26] Hose Y, Silva P, Seible F (2000): Development of a performance evaluation database for concrete bridge components and systems under simulated seismic loads. *Earthquake Spectra*, **16** (2), 413-442
- [27] FEMA P695 (2009): *Quantification of building seismic performance factors*. Federal Emergency Management Agency, Washington DC.
- [28] ATC-63, FEMA P695 (2009): *Quantification of building seismic performance factors*. Federal Emergency Management Agency, Washington DC
- [29] Jalayer F, Cornell CA (2003): A technical framework for probability-based demand and capacity factor (DCFD) seismic formats. *PEER-2003/08*, Pacific Earthquake Engineering Research Center, Berkeley, California.
- [30] Gupta A, Krawinkler H (2000): Dynamic P-delta effects for flexible inelastic steel structures. *Journal of Structural Engineering*, **126** (1), 145-154.